Simulation of Overhead Crane Wire Ropes Utilizing LS-DYNA®

Andrew Smyth, P.E.
LPI, Inc., New York, NY, USA

Abstract

Overhead crane wire ropes utilized within manufacturing plants are subject to extensive cyclic loading due to near continuous service operation. An LS-DYNA model was developed to assist in determining the expected fatigue life of the crane wire ropes by calculating both the dynamic cyclic stress and the total number of bending reversals per lift.

Since very complex contact conditions exist between the one-dimensional (1D) wire rope and the three-dimensional (3D) drum and sheaves it was determined that the LS-DYNA explicit solver was the preferred software for the dynamic simulation of the crane operation due to the robust contact algorithms and material capabilities within the code. Most implicit FEA codes would have convergence difficulty due to the contact between a concave surface and the 1D cable elements used to represent the wire rope. In addition, LS-DYNA also had the appropriate material model for bending resistance to be accurately represented within the 1D cable elements.

LS-DYNA simulations of the lifting operation determined the cyclic axial and bending stresses and the total number of reversals per lift. Using plant operating data and the appropriate fatigue curves allowed the expected fatigue life of the individual wire ropes to be calculated.

1-Introduction

Overhead cranes are widely utilized within manufacturing plants to lift and transport large payloads. Typical overhead cranes ride along bridge girders that traverse along a runway beam. The trolley frame rides along the bridge girders and contains the components important to the fatigue analysis of the wire ropes, namely the drum and sheave. An example image of a typical overhead crane is shown in Figure 1 (figures of the actual crane analyzed were not included for proprietary reasons).

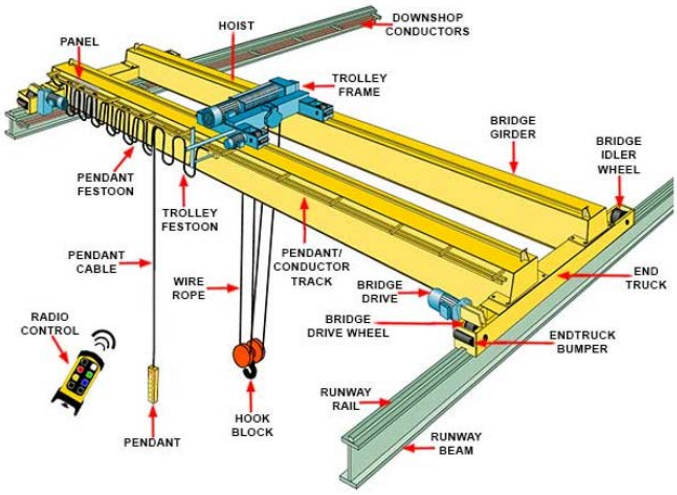

Figure 1: Overhead crane example image (from [1])

Critical to an overhead crane's operation and safety is the performance of the wire rope. A wire rope failure is a safety hazard to shop floor personnel and can potentially cause severe damage to both the crane and the payload. To this end, the fatigue life of an overhead crane wire rope was calculated for typical service operation, taking into account any dynamic axial and bending stresses experienced by the wire. For the specific overhead crane of this study, it was assumed that the payload was 44.3 metric tons and that the crane was in operation 365 days per year.

2-Model Development

2-1 Geometry

To simulate the performance of a wire rope during operation of an overhead crane it was necessary to model all portions of the crane structure that interact with the wire rope, including the drum, upper block and upper sheaves, as shown in Figure 2.

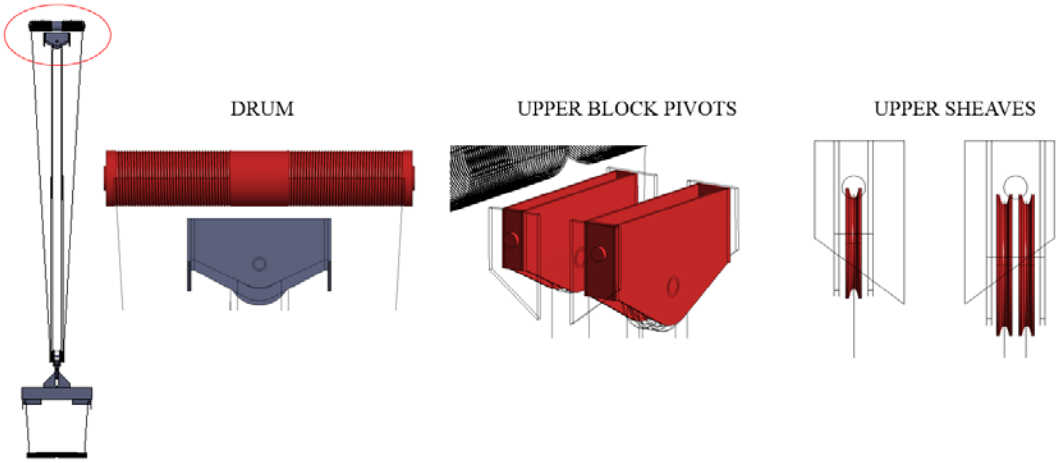

Figure 2: Overhead crane geometric model - drum, upper block, and upper sheaves

In addition, the lower block, lower sheaves and the payload were modeled as shown in Figure 3.

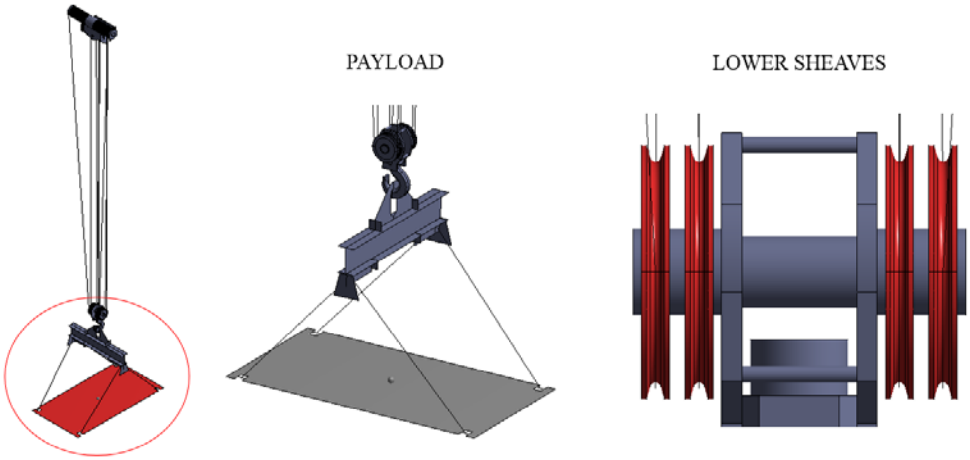

Figure 3: Overhead crane geometric components - lower block, lower sheaves, and payload

For the overhead crane detailed in this paper the payload was represented by a dummy density-free plate with a point mass attached such that parametric simulations could be performed varying the payload mass and center-of-gravity (CG).

2-2 LS-DYNA Finite Element Model

After creation of the geometric representation of the overhead crane it was necessary to develop a suitable finite element (FE) mesh for the explicit LS-DYNA simulations using ANSYS as shown in Figure 4.

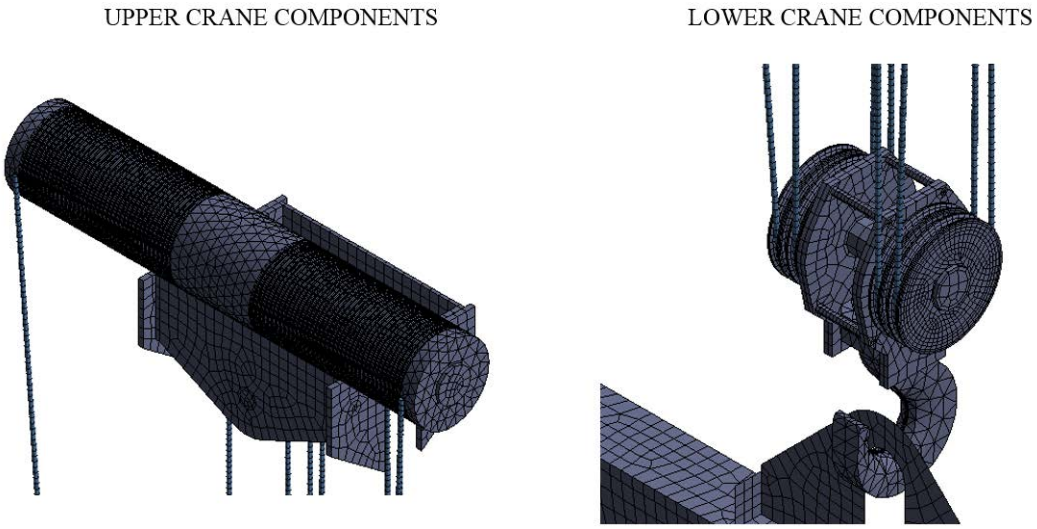

Figure 4: FE mesh discretization

The wire rope was modeled as a one-dimensional (1D) cable element using the LS-DYNA resultant beam formulation (ELFORM = 2) with the remaining overhead crane components modeled as rigid three-dimensional (3D) solids (ELFORM = 1 or 10, depending on the shape) and the payload modeled using two-dimensional (2D) shells (ELFORM = 2), 1D cable elements (ELFORM = 6) for the straps, and a mass element (*ELEMENT_INERTIA). The most important characteristics of the mesh pertained to the contact interfaces between the wire rope and the grooves, therefore specific attention was paid to the mesh on the drum grooves and the sheaves such that appropriate wire rope contact was maintained as shown in Figure 5.

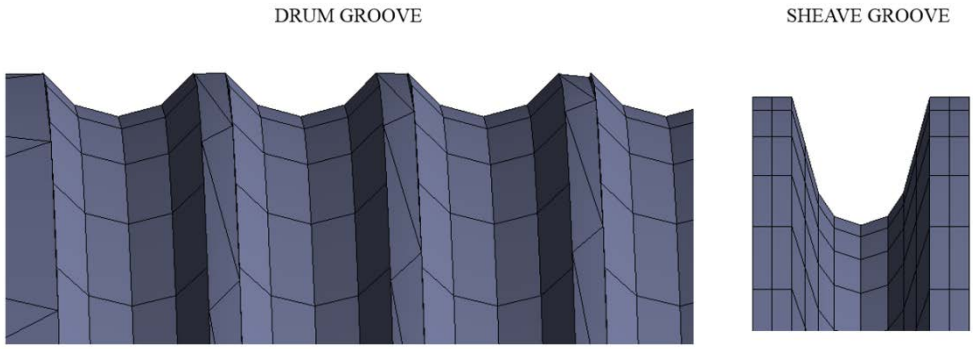

Figure 5: Localized FE mesh near grooves

3-Material Parameters

For the overhead crane simulations the material models utilized by both the rigid crane components and the payload shell elements were typical of structural steel and will not be detailed in this paper. Likewise, the payload strap properties were assumed to be typical of nylon. The critical material parameters for the simulations detailed in this paper were the wire rope properties, rigid body material damping, and wire rope damping.

3-1 Wire Rope Properties

One of the more important considerations when using LS-DYNA to perform the overhead crane simulations was the 1D resultant beam element's ability to include bending stiffness within a cable-type element, described in [2] and [3]. Using the *MAT_MOMENT_CURVATURE_BEAM material model (*MAT_166) allowed the beam to behave in a manner typical of a wire rope where some amount of both bending and torsional stiffness can be considered. In typical 1D cable elements only axial stiffness is accounted for. Using the known wire rope properties obtained from the wire rope data sheet allowed the axial force-strain, moment-curvature, and torque-twist rate curves to be developed for the *MAT_166 material model. A summary of the wire rope input data and derived properties is shown in Table 1 below.

Table 1: Wire Rope Properties

Wire Rope Data	
UTS (N/mm^2)	1960
Length (m)	109
CBL (kN)	422.2
MBL (kN)	359.4
OD (mm)	20
weight (lbm/ft)	1.24
fill factor	0.686
weight factor	0.86
spin factor	0.85

Derived Properties	
UTS (psi)	284274
CBL (lbf)	94914
MBL (lbf)	80796
Elastic modulus - rope (psi), assumed fill_factor*steel_modulus	19894000
OD (in)	0.787
Cross-sectional area (in.^2)	0.487
Tensile/Shear area (in.^2), assumed fill_factor*cross-sectional area	0.334
Density (lbm/in^3)	0.212
Ixx = Iyy (in.^4)	0.019

Using an assumed yield force of 50,000 lbf and a failure strain of 10% allowed a bilinear axial force-true strain curve to be developed, as shown in Figure 6 below.

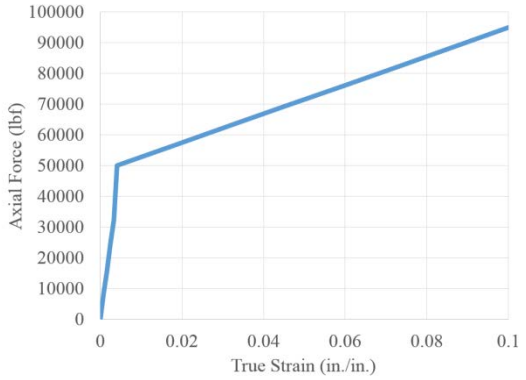

Figure 6: Wire rope material curve - axial force vs. true strain

Since actual bending stiffness data was not known for the subject wire rope the curve described in [2] was scaled appropriately using the relative stiffness ratios between the wire ropes, with the following moment-curvature curve implemented into LS-DYNA as shown in Figure 7.

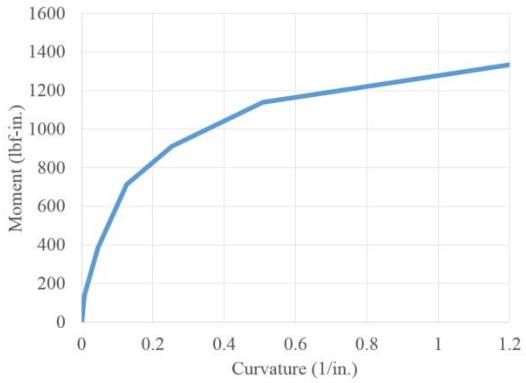

Figure 7: Wire rope material curve - moment vs. curvature

Similarly, the torque-twist relationship was taken directly from [3] as shown in Figure 8 below:

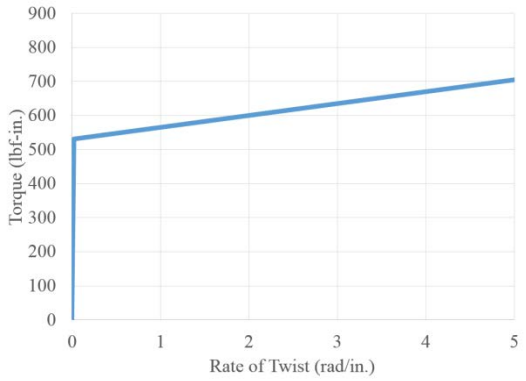

Figure 8: Wire rope material curve - torque vs. rate of twist

3-2 Lower Block Damping

To develop appropriate proportional (Rayleigh) damping coefficients (described in [4]) for the structural steel components, mainly the lower block and sheaves, it was necessary to perform hand calculations to estimate the natural frequency of the lower block hanging from the wire ropes. This was done by representing the system as a 1D oscillating point mass attached to a spring. Using equations described in [5] the vertical natural frequencies were calculated to be 3.9 Hz and 7.9 Hz, at a lift height of 40 feet and 10 feet, respectively. Combining these natural frequencies and an assumed critical damping ratio of 0.12, per [3], the Rayleigh damping coefficients were calculated according to the relationships described in [4]. Table 2 provides a summary of the rigid body damping input and displays the relevant mass and stiffness damping coefficients for input into the structural steel material models. It should be noted that the critical damping coefficients ($\zeta = 1$) are also shown and were used in the quasi-static stress initialization phase detailed in Section 5-Results.

Table 2: Rigid Body Damping Coefficients

INPUTS - VERTICAL OSCILLATION			
Mass - (lbm)	Length (ft)	Stiffness (lbf/in.) K - single rope	Stiffness (lbf/in.) K - 8 rope group
100000	40	20182	161456
	30	26909	215274
	20	40364	322911
	10	80728	645823

Proportional (Rayleigh) Damping				
Frequency (Hz)	Frequency (rad/sec)	Critical Damping Ratio	Mass Damping (Alpha)	Stiffness Damping (Beta)
3.975	24.98	0.12	4.00	0.0032
7.951	49.95	0.12		
3.975	24.98	1	33.30	0.0267
7.951	49.95	1		

3-3 Wire Rope Damping

The most important damping parameters for the overhead crane simulations performed were the damping coefficients of the wire rope elements. With no, or inappropriate, damping coefficients the 1D resultant beam element behaved in an unstable manner and a solution was not possible, even with LS-DYNA's robust solver capabilities. Since a zero damping solution was not feasible due to the aforementioned instabilities, it was not possible to utilize LS-DYNA to estimate the period and, therefore, the natural frequency of the wire rope during operation. To this end, a method described in [6] calculating the surge frequency for a helical spring was implemented to analytically represent the behavior of the wire rope damping. From this methodology the first two harmonic natural frequencies of the wire rope were calculated to be 99 Hz and 297 Hz. Table 3 summarizes the appropriate inputs and the Rayleigh coefficient output for the assumed damping ratio and critical damping.

Table 3: Wire Rope Damping Coefficients

INPUTS - ROPE SURGE	
Mass/length (lbm/in)	0.1033
Single rope strand mass (lbm)	50
Single rope stiffness (lbf/in)	20182

Proportional (Rayleigh) Damping				
Frequency (Hz)	Frequency (rad/sec)	Critical Damping Ratio	Mass Damping (Alpha)	Stiffness Damping (Beta)
99.129	622.84	0.12	112.11	0.000096
297.386	1868.53	0.12		
99.129	622.84	1	934.27	0.000803
297.386	1868.53	1		

4-Loads and Analysis Inputs

To effectively simulate the wire rope operation appropriate loads, boundary conditions, and contact parameters were needed. The overhead crane drum is driven by a motor attached to the movable trolley. All loading imparted to the wire rope is a function of the drum's rotational speed and the payload parameters. Also critical to the simulations was the contact interface between the 1D wire rope and the 3D solid elements.

4-1 Drum Loading

When in operation, overhead crane lifting and lowering is typically controlled manually by an operator such that the exact drum rotational velocity is not known. The plant provided an estimate for the typical vertical payload lifting velocities, based on observation of the lift height and lift time. Vertical linear velocity can then be converted into a rotational velocity for the drum based on the equations shown in [5] and summarized in Table 4.

Table 4: Drum Loading

INPUTS	
Drum Minor Diameter (mm)	400
Wire Rope Diameter (mm)	20
Vertical Drop (ft)	40

DERIVED INPUTS	
Drum Minor Diameter (in.)	15.75
Wire Rope Diameter (in.)	0.79
Pitch Diameter (in.)	16.54
Vertical Drop (in.)	480

OUTPUT			
Linear Velocity (in/s)	Lift Time (s)	Angular Velocity (rad/s)	RPM
4	120	-0.4838	-4.62
8	60	-0.9676	-9.24
16	30	-1.9352	-18.48
32	15	-3.8705	-36.96

On both drum ends the wire rope is fixed to the drum as shown in Figure 9 such that rotation of the drum causes the wire rope to wind about the drum through the grooves. Typically for this type of overhead crane with a grooved drum the wire rope does not stack allowing only one wire rope strand per groove.

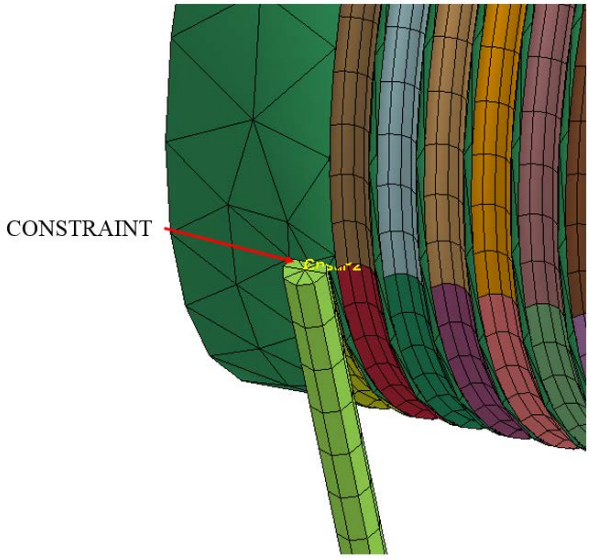

Figure 9: Wire rope attachment to the drum (symmetric)

4-2 Boundary Conditions

For the initial simulations it was assumed that the overhead crane was fixed in lateral space (lifting can occasionally occur with some lateral motion according to the plant). This fixity occurred at two locations, the drum and the upper sheave pivots. The drum was fixed translationally and was given a prescribed rotational velocity as described in 4-1 Drum Loading. The upper sheave pivots were also fixed translationally and were given the freedom to rotate about their axis using the concept of joints (*JOINT_COOR_REVOLUTE) to represent their interaction with the upper support housing.

4-3 Contact Parameters

A critical input into the overhead crane simulations was the contact definition between the 1D beam elements and the 3D solid elements. This was one of the deciding factors when electing to utilize LS-DYNA for the simulations, as opposed to a more conventional implicit FEA code. The robust contact capabilities within LS-DYNA allowed for an accurate representation of the contact between a sliding wire rope and the sheaves/drum, as shown in Figure 10 where the wire rope has begun to wrap around the drum during the lift.

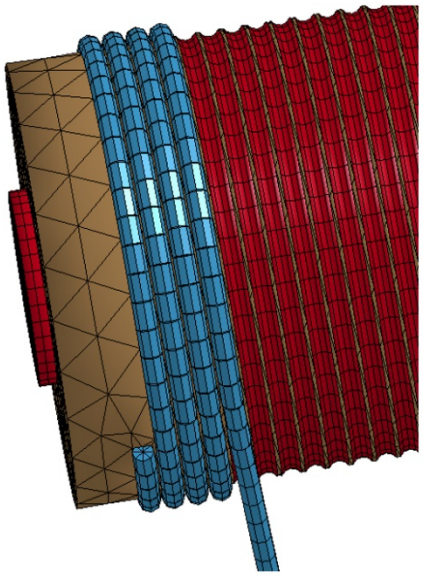

Figure 10: Contact representation – wire rope wrapping around drum grooves

To facilitate the wire rope to groove contact the *AUTOMATIC_NODES_TO_SURFACE card was utilized with a viscous damping coefficient of 0.12. Since the wire rope is greased, a static frictional coefficient of 0.15 was assumed with an exponential decay of 2 and a dynamic frictional coefficient of 0.05.

5-Results

Simulations of the operation of a wire rope utilized within an overhead crane were performed within LS-DYNA to calculate the number of bending reversals and the dynamic bending stress for input into a fatigue life calculation.

5-1 Stress Initialization

Before applying the drum rotational velocity it was necessary to initialize the gravity load such that the system achieved a steady-state, removing any dynamic effects due to gravity. This was done by applying the gravity load only with the critical damping parameters described in Table 2 and Table 3. After approximately 1.5s the system achieved steady-state with a constant vertical displacement of the payload and lower block and a relatively consistent 12,500 lbf axial tension along the length of the entire wire rope (as predicted by strength-of-materials calculations).

5-2 Payload Lifting Simulations

A typical payload lift height of 40 feet necessitated a comparatively (by LS-DYNA's standards) long run time of 80s, depending on the drum rotational speed, to achieve the full lift height. To limit the numerical error build-up over the large number of iterations the double precision solver was implemented. Snapshots over time shown in Figure 11 display the position of the lower block (with payload removed) as it is lifted to the final height.

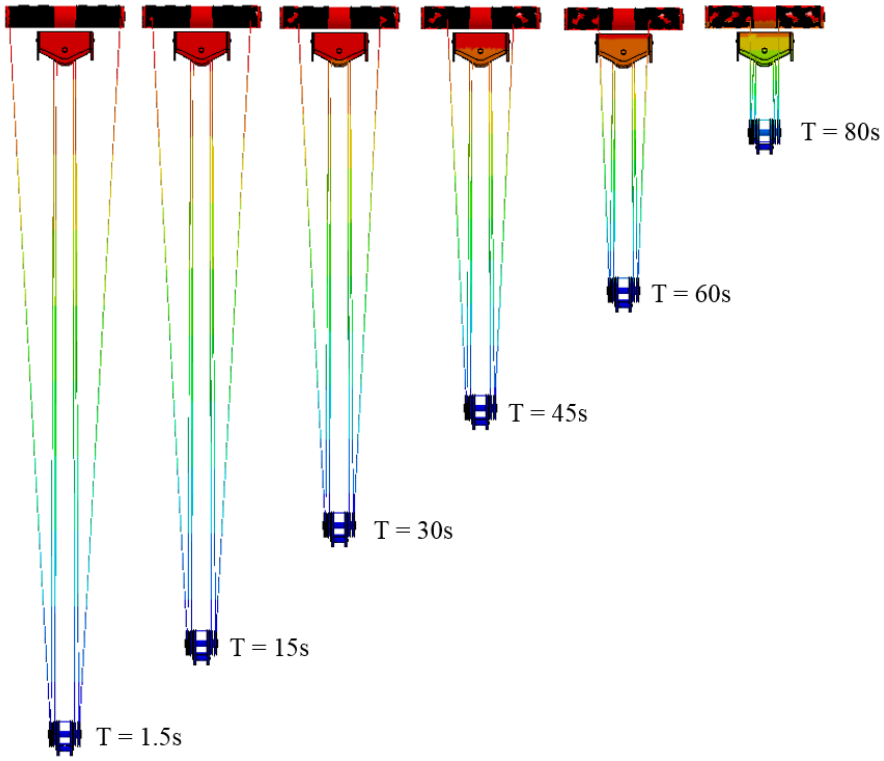

Figure 11: Lower block location as a function of time

To determine the total number of bending reversals per lift, various nodal locations along the wire rope were strategically selected for tracking with Figure 12 displaying the subject tracking node of the subsequent fatigue calculations.

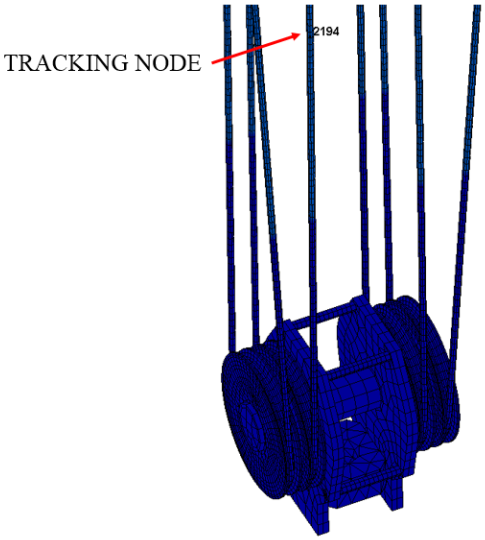

Figure 12: Tracking node for fatigue calculations

To calculate the number of reversals for each tracking node, the local minimum and maximum were summated from a time history plot of the vertical (y-axis) coordinate, shown in Figure 13 for the subject tracking node of this paper.

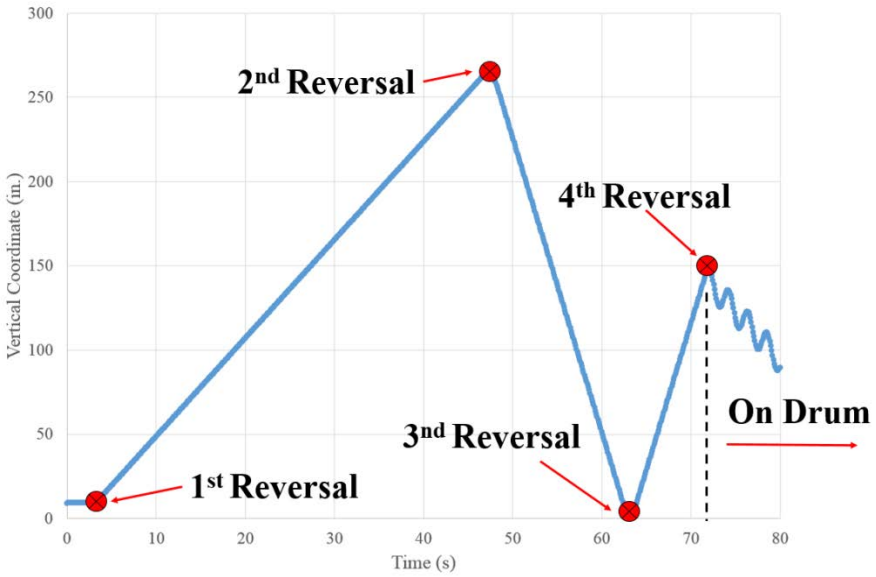

Figure 13: Tracking node 2914 bending reversal count

The bending reversal count, multiplied by 2 to consider lowering of the payload, gives the number of bending cycles per lift. Based on continuous crane operation with 2 lifts per hour the number of cycles per year was estimated to be 297,840. Since frictional contact was included between the rope and the drum/sheaves each bending reversal will also include an axial stress cycle as some of the wire rope tension is taken up by friction.

The second input into the fatigue life calculations is the cyclic stress components of the wire rope, both axial and bending, as it is pulled around the sheaves and the drum. During crane operation both the maximum and the minimum axial stresses will occur when the rope is wrapped around the drum with the axial stress steadily decreasing as the drum rotates, as shown in Figure 14.

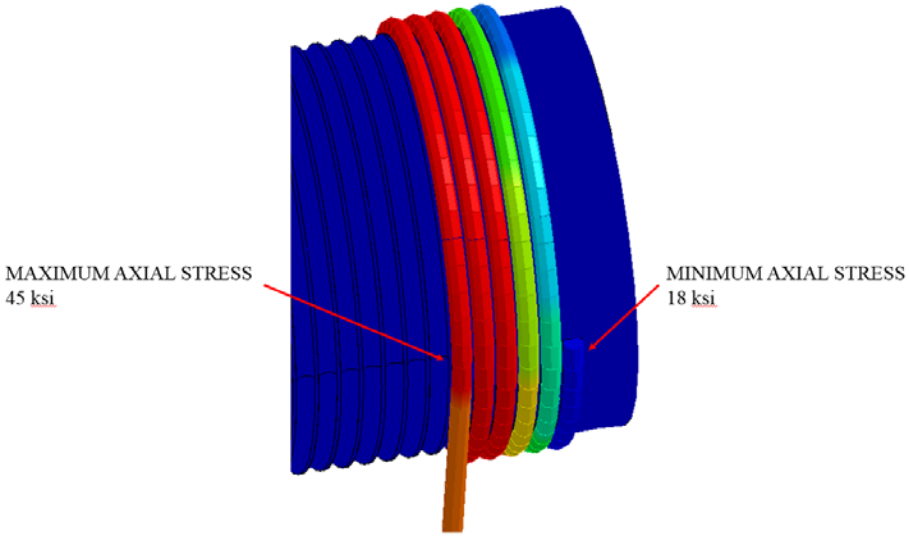

Figure 14: Wire rope axial stress

During operation, the maximum bending stress in the wire ropes also occurs as the rope begins to wrap around the drum and then is held constant as the wrapping continues. Figure 15 displays the maximum bending stress in the wire rope at the onset of drum wrapping.

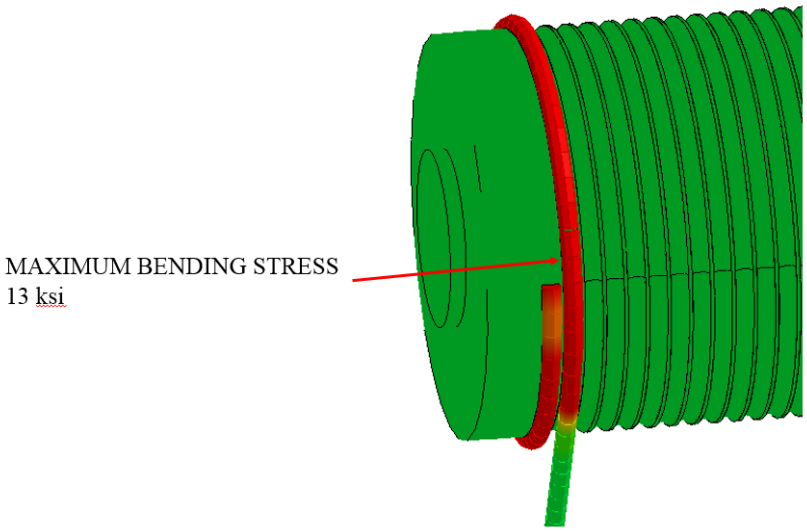

Figure 15: Wire rope bending stress

5-3 Fatigue Life Calculations

After calculating the number of reversals and the stress magnitudes for the wire rope during a typical lift operation using LS-DYNA, the fatigue life of the wire rope could be estimated using an appropriate fatigue life curve. A typical wire rope's fatigue strength is governed by the strength of the steel strands such that a steel fatigue life curve could be utilized within the calculations as shown in Table 5.

Table 5: Fatigue Life Calculations

INPUTS		
Tensile Strength	UTS (ksi)	284
Fatigue Coefficient	A (ksi)	10.4
	lift/hr	2
	lift/yr	17520
Yearly Cycles	N/yr	297840

OUTPUT										
Cycle Description	Cycles (n)	γ	Stress (ksi)					Goodman Stress (ksi)		
			Min.	Max.	Range	Alt.	Mean	Alt.	Mean	$\gamma\sigma^3$
Dead Weight Tension	1	0.06	0	45	45	22	22	24	49	6823
Tension Reduction @ Drum/Sheave (Raise)	4	0.24	18	45	27	14	31	15	30	6601
Tension Reduction @ Drum/Sheave (Lower)	4	0.24	18	45	27	14	31	15	30	6601
Bending @ Drum/Sheave (Raise)	4	0.24	0	13	13	7	7	7	14	613
Bending @ Drum/Sheave (Lower)	4	0.24	0	13	13	7	7	7	14	613
	17									

FATIGUE LIFE	
Equ. Alt. Stress (ksi)	28
Life (Cycles)	1182031
Life (years)	**3.97**

From the fatigue life calculations the wire rope would be expected to have a service life of approximately 4 years which is in-line with typical industry practice to replace heavy service wire ropes every few years.

6-Conclusions

The service fatigue life of an overhead crane's wire rope was calculated using inputs from LS-DYNA simulations. Using the specialized material models developed for use with 1D beams allowed the wire rope's behavior to be accurately represented in the overhead crane simulations. In addition, the robust contact capabilities enabled the contact between 1D line bodies and 3D solid bodies to be captured. Traditional implicit FEA codes are not well suited to this type of contact condition and convergence would be very difficult. LS-DYNA allowed for an accurate simulation of an overhead crane's operation and generated appropriate inputs for a downstream wire rope fatigue life calculation.

References

[1] "Crane Parts and Crane Components: Overhead crane parts, gantry crane parts, jib crane parts." Retrieved from http://www.cranesdq.com/cranes-and-crane-parts.html, October 2015

[2] Stolle, C., and Reid, J. "Modeling Wire Rope Used in Cable Barrier Systems," 11th International LS-DYNA Users Conference, June 2010.

[3] Reid, J. "Development of Advanced Finite Element Material Models for Cable Barrier Wire Rope," Mid-America Transportation Center, Report # MATC-UNL:220, August 2010.

[4] Meirovitch, L. "Fundamentals of Vibrations," McGraw-Hill, New York, NY, 2001

[5] Lindeburg, M., "Mechanical Engineering Reference Manual for the PE Exam,", 12th Edition, PPI, Inc., 2006

[6] "Surge frequency of a spring." Retrieved from http://www.roymech.co.uk/Useful_Tables/Springs/Springs_Surge.html, May 2009